Journal of Applied Electrochemistry **32**: 389–394, 2002.

Influence of an electrochemically generated gas phase on pressure drop in a three-dimensional electrode and an inert bed

S.M. ŠERBULA* and V.D. STANKOVIĆ
Technical Faculty in Bor, University of Belgrade, VJ 12, 19210 BOR, Yugoslavia
*(*author for correspondence, e-mail: sherbula@ptt.yu)*

Received 19 February 2001; accepted in revised form 6 February 2002

Key words: gas–liquid–solid, inert bed, packed bed, pressure drop, three-dimensional electrode, two-phase flow

Abstract

The influence of an electrochemically generated gas phase on the pressure drop in a three-dimensional electrode and an inert bed has been investigated. The electrode was composed of silvered glass particles, whereas the inert bed was composed of glass particles of the same diameter. During water electrolysis smaller gas bubbles are generated than by introducing gas into the system by means of a fluid distributor. Electrochemically generated bubbles with the liquid phase circulate upward through the electrode and the inert bed. The pressure drop for a monophase fluid was measured, as well as the change of pressure drop with time in the electrode and the inert bed for two-phase flow of fluid through an electrochemical cell. The steady and unsteady periods of the change of pressure drop have been discussed. Experiments were carried out at different electrolyte velocities and for different current densities. Higher electrolyte velocities cause an increase in the pressure drop in both beds. Also, increased current density causes an increase in gas evolution intensity at the electrode thereby increasing the pressure drop in both beds. A mathematical model describing the change of pressure drop with time has been proposed. The proposed model showed good agreement with experimental results as well as the results from the literature.

List of symbols

d	particle diameter (mm)
i	current density (A m^{-2})
i_{cal}	current density of the current feeder for calculated pressure drop (A m^{-2})
L	height of the bed (m)
k	constant (s^{-1})
w_g	gas evolution intensity at surface of 3D electrode (m^3 m^{-2} s^{-1})
w_l	electrolyte velocity in the electrochemical cell (m s^{-1})
ΔP	pressure drop in the bed (kPa)
ΔP_0	initial pressure drop in the bed (kPa)
ΔP_{st}	pressure drop in the bed in the steady period (kPa)
ΔP_1	pressure drop in the three-dimensional electrode (kPa)
ΔP_2	pressure drop in the inert bed (kPa)

Greek symbols

ε_g	gas hold-up
ε_l	liquid hold-up
ε_s	solid hold-up
φ_g	volume fraction of the gas in the liquid
μ_g	gas viscosity (Pa s)
μ_l	liquid viscosity (Pa s)
ρ_g	gas density (kg m^{-3})
ρ_l	liquid density (kg m^{-3})
τ	time (min)

1. Introduction

The three-phase gas–liquid–solid system is frequently encountered in hydrometallurgy, electrometallurgy, chemical engineering, biochemical engineering as well as other fields [1]. Reactors with a fixed bed through which a two-phase gas–liquid flow circulates are frequently used in chemical, electrochemical and biochemical engineering [2–4]. Reactors with three-dimensional (3D) electrodes are used for electrochemical deposition of metals from dilute solutions [5]. Simultaneously with electrodeposition of metal a gas phase often evolves at the surface of the 3D cathode [6,7]. Electrochemically generated gas circulates upward along with the continuous liquid flow [8] over the inert bed composed of particles of the same size as the 3D electrode. It is necessary to know the hydrodynamic characteristics of the two-phase gas–liquid fluid through both beds

(3D electrode and inert bed) to apply the three-phase system in industry adequately [9–12].

The aim of this work is to investigated the hydrodynamic characteristics of the three-phase gas–liquid–solid system in an electrochemical cell in which, during water electrolysis, the gas phase is generated in the form of bubbles at the 3D cathode. The solid phase consists of silvered spherical glass particles ($d = 2$ mm) which are in contact with a current feeder comprising together the 3D electrode. In addition, the solid phase also comprises an inert bed composed of glass particles of the same diameter as the electrode. The inert bed was positioned above the 3D electrode. The hydrodynamic characteristics of the three-phase system have been examined as influenced by: gas evolution intensity, electrolyte velocity, the size of the particles composing the 3D electrode and the inert bed, geometrical characteristics of the electrochemical cell, the gas hold-up in both beds etc. The hydrodynamic characteristics of the two-phase gas–liquid flow have been examined in both beds and a mathematical model has been formulated of the influence of the generated gas phase on the pressure drop through both beds. The model comprises the unsteady and steady period of the two-phase fluid flow through the beds.

2. Experimental details

Experiments were carried out using the experimental set up shown in Figure 1. The experimental set-up consisted of an electrochemical cell, a reservoir, a centrifugal pump, a flowmeter, piezometric tubes, a 3D electrode and an inert bed. The electrochemical cell used was made of Plexiglass and was of rectangular cross-section (135 mm × 100 mm and 450 mm height). The electrochemical cell was divided vertically by a porous plastic diaphragm. The diaphragm separated the anode from the cathode compartment. A fluid distributor was inserted in both compartments having the function of a bed bearer in the cathode compartment. Only an electrode made of a flat lead sheet was inserted in the anode compartment. The current feeder was made of a stainless steel sheet (87 mm × 87 mm × 2 mm) and was vertically placed, parallely to the wall of the cell. The cathode compartment (20 mm × 87 mm × 87 mm) between the current feeder and the diaphragm was filled with silvered glass beads 87 mm high and 20 mm wide. These particles, being a fixed bed connected to the current feeder, formed the 3D electrode. Over the conductive bed an inert bed was placed composed of particles of the same size as those forming the 3D electrode.

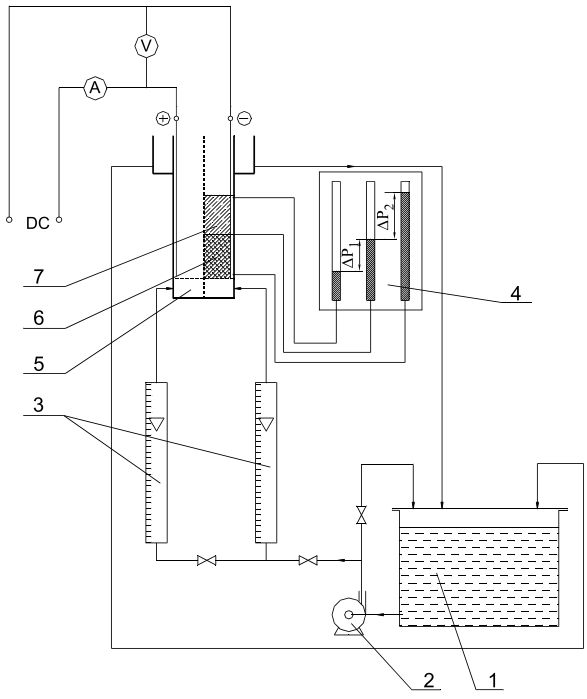

Fig. 1. Experimental set-up: (1) reservoir, (2) centrifugal pump, (3) flowmeters, (4) piezometric tubes, (5) rectangular electrochemical cell, (6) 3D electrode and (7) inert bed.

The pressure drop in both beds was periodically measured on the basis of the difference in the levels in piezometric tubes. The openings for connection of the piezometric tubes were situated at the lower and the upper part of each bed. The first opening was situated above the fluid distributor but at a distance of 25 mm from the distributor to avoid the influence of the distributor and to enable an even distribution of the electrolyte in the 3D electrode. The next opening was situated exactly on the boundary between the two beds: 3D electrode and inert bed. The difference in the levels of liquid in these two piezometric tubes represents the pressure drop in the 3D electrode. The next opening to which a piezometric tube was attached was situated immediately below the top of the inert bed. The difference in the levels of liquid in the tube between this attachment and that on the boundary between the two beds gives the pressure drop in the inert bed.

Silvered glass particles were introduced into the cell occupying the cathode compartment between the electrolyte distributor, the diaphragm and the flat cathode. The 3D cathode formed in this way was 77 mm high. A bed of glass particles of the same size as those composing the 3D electrode was then formed above the active bed. This bed was 90 mm high. Glass particles of medium size (dia. 2 mm, glass density 2512 kg m^{-3}) were used. The porosity of a bed of spherical particles (dia. 2 mm) is 0.38. The reservoir was filled with 11.3×10^{-3} m^3 of 0.5×10^3 mol m^{-3} H_2SO_4 solution. The experiment was started by switching on the centrifugal pump and the same liquid phase flow was regulated through both anode and cathode compartments. When the system became balanced, with no oscillations of the flow, the pressure drop was measured in the 3D electrode and inert bed without the gas phase. The d.c. feeder and the chronometer were than simultaneously switched on. Consequently, water electrolysis and the evolution of hydrogen bubbles at the 3D cathode took

place in the cell. The pressure drop values through both beds increased and were determined every 2 min until the steady state was reached. Then the d.c. feeder was switched off first, in order for the liquid phase to flow for a certain time and completely remove hydrogen bubbles left behind in the pores of the bed. When there were no more free bubbles in the electrolyte, the centrifugal pump was switched off and the liquid phase remained in the cell in preparation for the next experiment.

3. Results and discussion

The pressure drop in the 3D electrode and the inert bed increases when water electrolysis and evolution of hydrogen bubbles at the 3D electrode takes place. Hydrogen bubbles partly remain in the space between the particles of the 3D electrode, and are partly carried along by the continuous liquid phase circulating upward through the inert bed. A typical plot of pressure drop per unit bed height, against time for 3D electrode and inert bed is presented in Figure 2. The pressure drop increases steeply, following cell switch-on, and then tends to a constant value depending on the applied current density (calculated on the feeder surface) and the hydrodynamic conditions in the bed. The experimental results in Figure 2, imply the existence of two process periods in which the pressure drop behaves differently, namely, in the initial unsteady period, where there is a strong dependence of $\Delta P/L$ with time and the second, steady period. The 3D electrode exhibits a higher pressure drop than the inert bed, as shown in Figure 2 [13].

Based on Faraday's laws and the 'equation of continuity' it is possible to determine gas evolution intensity on the 3D electrode, as well as gas velocity through the inert bed [13, 14].

Figure 3 shows the change of pressure drop per unit height of the 3D electrode $(\Delta P_1/L)$ with time for different electrolyte velocities at a constant current density of 400 A m^{-2} and for particles of diameter 2 mm.

On switching the current on water electrolysis takes place. The generated hydrogen carried along by the liquid flow partly passes through the 3D electrode whereas the remaining part remains in the space between the silvered glass particles. The hydrogen remaining in the 3D cathode reduces the space through which the electrolyte flows thus increasing resistance to electrolyte flow. The resistance to the two-phase gas–liquid flow is directly proportional to the quantity of hydrogen hold-up in the porous bed [1, 13, 14].

This results in an increase in the pressure drop through the bed with increased gas hold up. Hydrogen hold-up in the bed increases only in the first few minutes as shown in Figure 3. For each electrolyte velocity there is a maximum hydrogen hold-up in the bed and this value defines the steady state. In the steady period all the hydrogen generated at the electrode leaves its surface because the bed is saturated with hydrogen bubbles. With increasing electrolyte velocity there is an increase in the pressure drop per unit bed height. Figure 4 shows the change in pressure drop per unit bed height with time for different electrolyte velocities at a constant current density of 400 A m^{-2}.

It is obvious that the pressure drop per unit bed height in the inert bed increases with time. This implies that hydrogen bubbles, which circulate with the continuous electrolyte flow from the 3D electrode to the inert bed, remain in the space between the glass particles. The gas

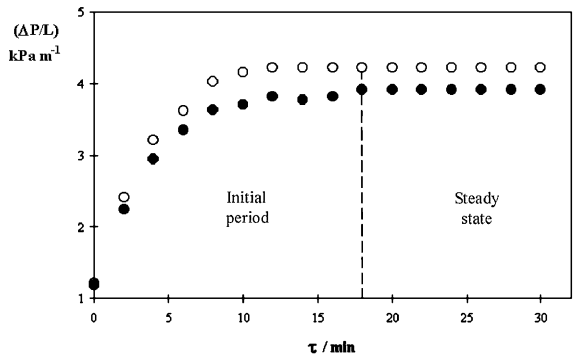

Fig. 2. Change of pressure drop per unit bed height against time, (○) 3D electrode and (●) inert bed.

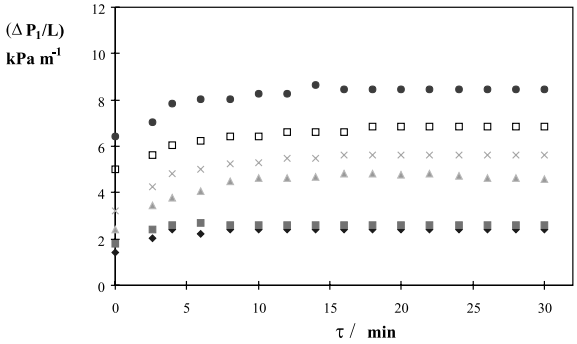

Fig. 3. Change of pressure drop per unit bed height against time in the 3D electrode for different electrolyte velocities (m s^{-1}): (◆) 0.0073, (■) 0.0109, (▲) 0.0128, (×) 0.0152, (□) 0.018, (●) 0.0215; $d = 2$ mm; $i = 400$ A m^{-2}.

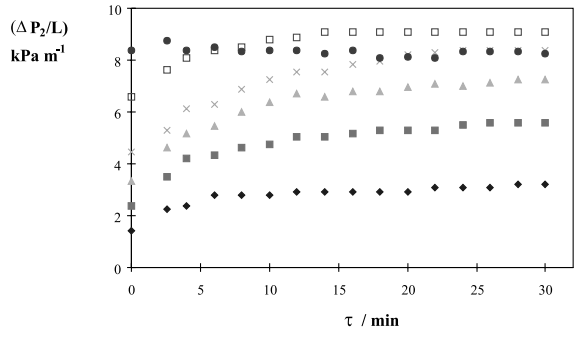

Fig. 4. Change of pressure drop per unit bed height against time in the inert bed for different electrolyte velocities (m s^{-1}): (◆) 0.0073, (■) 0.0109, (▲) 0.0128, (×) 0.0152, (□) 0.018, (●) 0.0215; $d = 2$ mm; $i = 400$ A m^{-2}.

hold-up increases with time until the steady state is reached. Furthermore, the pressure drop in the inert bed increases with increasing electrolyte velocity. At an electrolyte velocity of 0.0215 m s^{-1} there is no change of pressure drop per unit bed height with time. This velocity is close to the minimum fluidization velocity so that channels are formed in the bed through which the two-phase gas–liquid fluid circulates. This indicates that there is no resistance to flow and there is no change in pressure drop per unit bed height with time.

The shape of the curve showing the change of pressure drop in the bed with time during water electrolysis resembles the shape of a polarization curve. If, by analogy, we write the equation of the change of pressure drop per unit bed height, $\Delta P/L$, we obtain:

$$\frac{\Delta P}{L} = \frac{\Delta P_{st}}{L}(1 - e^{-k\tau}) + \frac{\Delta P_0}{L} e^{-k\tau} \quad (1)$$

The initial pressure drop value during circulation of the liquid phase only for time $\tau = 0$ through the bed is $\Delta P_0/L$. The pressure drop increases with time until the bed is saturated with gas bubbles, that is, until the steady state is reached $\Delta P_{st}/L$. For any set of experimental data ($\Delta P/L - \tau$), the constant k can be determined by taking the logarithm of equation giving the following form:

$$\ln\left(\frac{\Delta P - \Delta P_{st}}{\Delta P_0 - \Delta P_{st}}\right) = -k\tau \quad (2)$$

which in a physical sense represents the contribution to the pressure drop with time as a result of water electrolysis, that is, the contribution of the gas phase to the pressure drop per unit bed height. The constant k is a complex function of all physical characteristics of the three phases (solid, liquid and gas phase), liquid and gas velocity, gas volume fraction as well as the hold-up of each phase:

$$k = f(\rho_l, \rho_g, \mu_l, \mu_g, w_l, w_g, \varphi_g, d, \varepsilon_s, \varepsilon_l, \varepsilon_g) \quad (3)$$

The constant k is calculated from the rearranged experimental data, that is, from the slope of the straight line using Equation 2. After graphical determination of k, it is possible to examine the agreement of the experimental data with the proposed Equation 1.

Figure 5 shows linear dependence $\ln(\Delta P - \Delta P_{st}/\ \Delta P_0 - \Delta P_{st})$ on time τ, for the 3D electrode $w_l = 0.0073$ m s^{-1} and $d = 2$ mm.

As shown, the slope is different for the applied current densities which means that the steady state is not reached for the same time. The slope of the straight line (i.e., constant k) is a complex function of a great number of parameters (as indicated by Equation 3) and it is unrealistic to expect the steady state to be reached in proportionately the same time at different current densities. The constant k (graphically determined) was used for calculating the pressure drop in the 3D electrode by Equation 1. The constant k for the inert bed was determined likewise. Values of k are listed in Table 1 for all applied current densities.

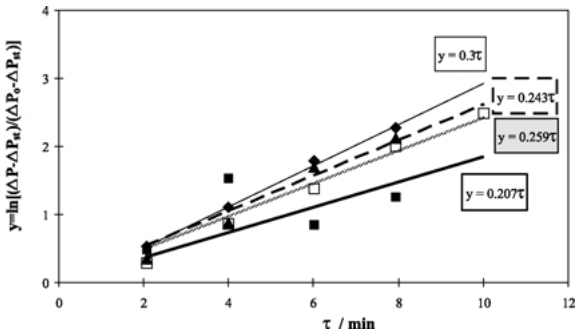

Fig. 5. Time-dependent logarithmic change in the pressure drop for the 3D electrode and different current densities (A m^{-2}): (◆) 200, (■) 400, (▲) 600, (□) 800; $d = 2$ mm; $w_l = 0.0073$ m s^{-1}.

Table 1. Values of constant k for the 3D electrode and inert bed at different current densities ($d = 2$ mm)

k/s^{-1}	Current density/A m^{-2}			
	200	400	600	800
3D electrode	0.3	0.207	0.243	0.259
Inert bed	0.115	0.190	0.307	0.343

Inspection of Table 1 reveals that k increases with increasing current density. The higher the current density, the higher the gas evolution intensity so that both beds are filled with bubbles more rapidly. Thus, with the higher value of the constant k, the steady period is attained more rapidly. The only exception is $k = 0.3$ s^{-1} for a current density of 200 A m^{-2} in the 3D electrode, where the steady state is reached quickly but the pressure drop rise is small (from 1 to 1.6 kPa m^{-1}). The influence of the rate at which the steady state is reached is almost negligible and cannot be measured precisely because the steady state is reached for two sets of data.

From these values of the constant we can calculate the pressure drop change per unit bed height for the applied geometric current densities ($i_{cal} = 200$, 400, 600 and 800 A m^{-2}) and compare them with the experimental values of the pressure drop per unit bed height as shown in Figures 6 and 7.

Figure 6 shows calculated values of the pressure drop per unit bed height by using Equation 1 for the applied geometric current densities 200, 400, 600 and 800 A m^{-2} in the 3D electrode, as well as experimentally obtained data for the pressure drop per unit bed height at the applied densities. Experimentally obtained data are represented as separate points, whereas calculated data are presented as a continuous line and marked i_{cal}, for the applied current densities. It can be seen from Figure 6 that experimental values for the pressure drop per unit height of the 3D electrode are arranged immediately around the linear dependence calculated by Equation 1 for the corresponding current density.

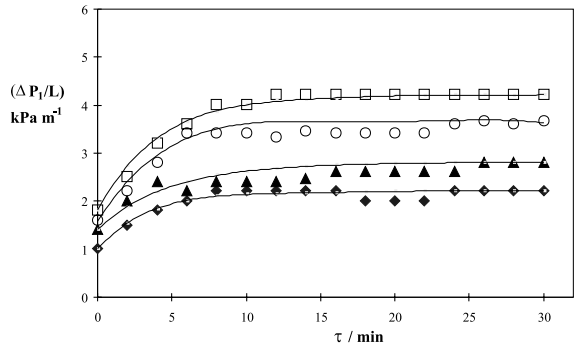

Fig. 6. Change of pressure drop per unit bed height against time in the 3D electrode, experimental data for different current densities (A m^{-2}): (◆) 200, (▲) 400, (○) 600, (□) 800, and calculated value (——) by Equation 1; $d = 2$ mm; $w_l = 0.0073$ m s^{-1}.

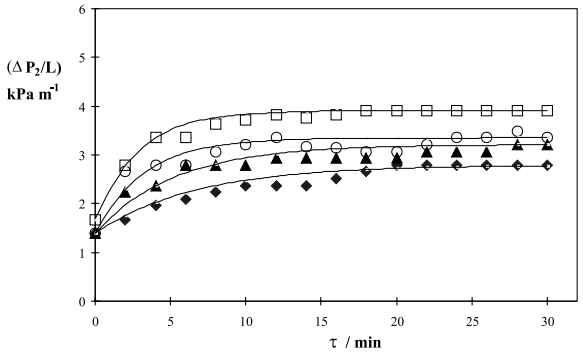

Fig. 7. Change of pressure drop per unit bed height against time in the 3D electrode, experimental data for different current densities (A m^{-2}): (◆) 200, (▲) 400, (○) 600, (□) 800, and calculated value (——) by Equation 1; $d = 2$ mm; $w_l = 0.0073$ m s^{-1}.

Figure 7 shows calculated values of the pressure drop per unit bed height for the applied current densities of 200, 400, 600 and 800 A m^{-2} as well as experimental data. Experimental data are indicated as distinct plots in Figure 7, whereas calculated values are represented as a continuous line and are marked i_{cal}, for the applied current densities. Figure 7 shows that experimental values of the pressure drop per unit bed height and calculated values of the dependence are in good agreement.

Both Figures 6 and 7 confirm the appropriateness of the chosen mathematical model which successfully describes the pressure drop change per unit bed height.

To test the proposed model for the description of the unsteady change of pressure drop in the bed (Equations 3 and 4), published data for the pressure drop in a 3D electrode were used [6].

Values of k for the 3D electrode composed of graphite particles for different current densities are given in Table 2. These values were determined graphically using the same method shown in Figure 5, that is, as a mean value of the direction coefficient from the set of experimental data, $\ln(\Delta P - \Delta P_{st}/\Delta P_0 - \Delta P_{st})$ and time τ.

Values of constant k (given in Table 2), as well as those for the 3D electrode of silvered spherical particles of $d = 2$ mm, increase with increasing current density with one exception which may be as experimental anomaly.

Table 2. Values of constant k for the 3D electrode composed of graphite particles at different current densities (d = 0.54 mm)

k/s^{-1}	Current density/A m^{-2}		
	270	811	1216
3D electrode graphite particles	0.175	0.313	0.22

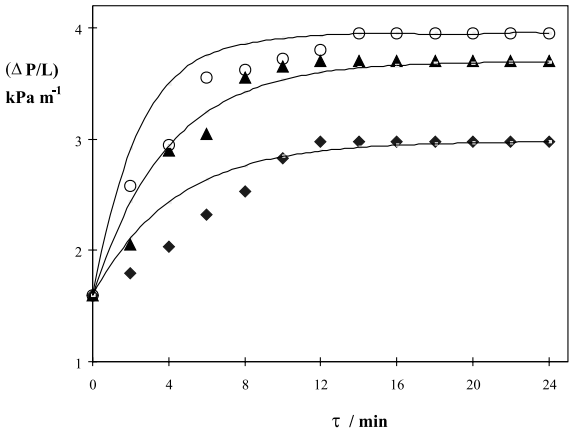

Fig. 8. Change of pressure drop per unit bed height against time in the 3D electrode, experimental data for different current densities (A m^{-2}): (◆) 270, (▲) 811, (○) 1216, and calculated value (——) by Equation 1; $d = 0.54$ mm; $w_l = 0.00197$ m s^{-1}.

Figure 8 shows experimental data (plots) for pressure drop per unit height of the 3D electrode and calculated values (continuous line) for different parameters, particle shapes and geometric current densities i_{cal}. These show good agreement of the chosen mathematical model, which adequately describes the unsteady and steady period.

4. Conclusion

An electrochemically generated gas phase influences the pressure drop increase in the 3D electrode and the inert bed. Gas hold-up increases with time in both beds and results in a pressure drop rise in both beds. In the steady state the bed is saturated with gas bubbles so that their quantity remains the same with time. With increased electrolyte velocity the pressure drop per unit height of both beds increases. For electrolyte velocities approaching the minimum fluidization velocity, the gas phase does not affect the pressure drop in the bed because the two-phase gas–liquid flow circulates through the channels formed in the bed. With increasing current density at the 3D electrode there is an increase in the intensity of gas evolution at the surface of the electrode, which results in a pressure drop rise in both the 3D electrode and the inert bed.

The proposed model describes the initial pressure drop per unit bed height and its change against time. The model shows good agreement with experimental results for both beds as well as some limited literature data.

References

1. L.S. Fan 'Gas–Liquid–Solid Fluidization Engineering' (Butterworths, Stoneham, MA, 1989).
2. U. Akman and A.K. Sunol, *Chem. Eng. Sci.* **49** (1994) 3555.
3. I. Iliuta, F.C. Thrion and O. Muntean, *Chem. Eng. Sci.* **51** (1996) 4987.
4. F. Larachi, M. Cassanello, A. Laurent, N. Midoux and G. Wild, *Chem. Eng. Process.* **36** (1997) 497.
5. D. Pletcher, I. Whyte, F.C. Walsh and J.P. Millington, *J. Appl. Electrochem.* **21** (1991) 667.
6. V.D. Stanković, G. Lazarević and A.A. Wragg, *J. Appl. Electrochem.* **25** (1995) 565.
7. V.D. Stanković and S. Stanković, *J. Appl. Electrochem.* **21** (1991) 124.
8. V.S. Stanković, R. Grujić and A.A. Wragg, *J. Appl. Electrochem.* **28** (1998) 321.
9. S.H. Chern, K. Muroyama and L.S. Fan, *Chem. Eng. Sci.* **38** (1983) 1167.
10. S.H. Chern, L.S. Fan and K. Muroyama, *AIChE J.* **30** (1984) 288.
11. L.S. Fan, K. Muroyama and S.H. Chern, *Chem. Eng. J.* **24** (1982) 143.
12. G.H. Song, F. Bavarian, L.S. Fan, R.D. Buttke and L.B. Peck, *Can. J. Chem. Eng.* **67** (1989) 265.
13. S.M. Šerbula, PhD thesis (University of Belgrade, 2000).
14. S.M. Šerbula and V.D. Stanković, *J. Serb. Chem. Soc.* **66** (2001) 53.